

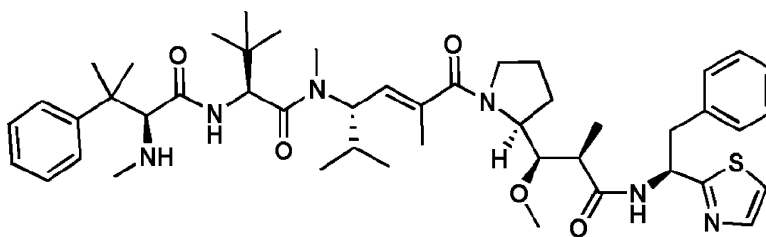
Article

## Hybrids of the Hemiasterlin Analogue Taltobulin and the Dolastatins Are Potent Antimicrotubule Agents

Arie Zask, Joshua Kaplan, Sylvia Musto, and Frank Loganzo

*J. Am. Chem. Soc.*, **2005**, 127 (50), 17667-17671 • DOI: 10.1021/ja053663v • Publication Date (Web): 22 November 2005

Downloaded from <http://pubs.acs.org> on March 25, 2009



### More About This Article

Additional resources and features associated with this article are available within the HTML version:

- Supporting Information
- Access to high resolution figures
- Links to articles and content related to this article
- Copyright permission to reproduce figures and/or text from this article

[View the Full Text HTML](#)

## Hybrids of the Hemiasterlin Analogue Taltobulin and the Dolastatins Are Potent Antimicrotubule Agents

Arie Zask,<sup>\*,†</sup> Joshua Kaplan,<sup>†</sup> Sylvia Musto,<sup>‡</sup> and Frank Loganzo<sup>‡</sup>

Contribution from Chemical and Screening Sciences and Oncology Research, Wyeth Research, 401 North Middletown Road, Pearl River, New York 10965

Received June 3, 2005; E-mail: zaska@wyeth.com

**Abstract:** The targeting of microtubules is an important mechanism for cancer chemotherapy. However, there is still a need for improved antimicrotubule agents. A number of seemingly structurally disparate peptidic natural products inhibit tubulin polymerization by binding to a region of the tubulin heterodimer close to the vinca binding site. An analogue of the naturally occurring tripeptide hemiasterlin, taltobulin (HTI-286, **3**), has advanced to clinical trials. Structure–activity relationship studies of **3** have revealed critical structural elements necessary for antimicrotubule activity that correspond to comparable groups in the amino terminus tripeptide region of the dolastatins. To investigate the structural relationship between the hemiasterlins and the more complex dolastatins, hybrid compounds composed of **3** and the carboxy terminus dipeptides of dolastatin 10, or the dolastatin 15 analogue cemadotin, were synthesized. The resulting hybrid compounds were potent antimicrotubule agents, thus establishing a structural relationship between the hemiasterlins and the dolastatins. This relationship may be useful in the design of analogues having improved activity in resistant cell lines expressing the P-glycoprotein transporter, for establishing structural relationships with other classes of peptidic antimicrotubule agents, or for modeling studies of the tubulin binding site of these agents.

### Introduction

The targeting of microtubules is an important mechanism for cancer chemotherapy with the taxanes (paclitaxel, docetaxel) and vinca alkaloids (vincristine, vinblastine, vinorelbine) of great utility in the clinic.<sup>1–3</sup> However, there exists an unmet need as current therapies suffer from limited extension of survival time due to inherent or acquired resistance which is often associated with expression of the P-glycoprotein drug transporter.<sup>4</sup> A plethora of promising antimicrotubule agents are currently in clinical and preclinical development.<sup>3</sup> These agents may stabilize microtubules, as do the taxanes, or destabilize them, as in the case of the vinca alkaloids. In either case, interference with microtubule dynamics prevents chromosomal separation, causing mitotic arrest and cell death (apoptosis). Microtubules are proteins comprised of heterodimers of  $\alpha$ - and  $\beta$ -tubulin, which bind the taxanes, vinca alkaloids, and colchicines in three distinct tubulin binding sites. Several peptide and depsipeptide natural product inhibitors (Figure 1) of tubulin polymerization have been shown, through competitive binding experiments, to bind in a site close to the vinca binding site.<sup>5,6</sup> These include dolastatin

10 (**1**), hemiasterlin (**2**), phomopsin, and cryptophycin 1. Taltobulin (HTI-286, **3**), a synthetic analogue of the naturally occurring tripeptide hemiasterlin, is a promising anticancer agent that has advanced to clinical trials.<sup>7</sup> It is a poor substrate for P-glycoprotein, and thus exhibits reduced multidrug resistance relative to paclitaxel and vincristine.<sup>8</sup> Several members of the dolastatin family of naturally occurring peptides and their analogues, including dolastatin 10 (**1**), TZT-1027 (auristatin PE, **4**), cemadotin (LU103793, **5**), and synthadotin (ILX651, **6**), are in clinical trials.

In the course of our investigations on the structure–activity relationships (SARs) of **3**,<sup>9</sup> we became interested in the structural relationship among the naturally occurring peptides that inhibit tubulin polymerization and also noncompetitively inhibit the binding of the vinca alkaloids to tubulin. Several studies attempting to establish a relationship among the tubulin binding peptidic natural products have met with limited success.<sup>10–13</sup> A recent modeling study using goodness of shape similar fit (GSSF) analysis proposed regions of overlap among eight of these structurally disparate peptides (including **1**, **2**, dolastatin 15 (**7**), phomopsin A, and cryptophycin 1) but was unable to identify a common continuous pharmacophore.<sup>10</sup> Similarly, a

<sup>†</sup> Chemical and Screening Sciences.

<sup>‡</sup> Oncology Research.

- (1) Rowinsky, E. K.; Tolcher, A. W. Antimicrotubule agents. In *Cancer Principles and Practice*, 6th ed.; Devita, V. T., Jr., Hellman, S., Rosenberger, S. A., Eds.; Lippincott Williams and Wilkins: Philadelphia, 2001; pp 431–452.
- (2) Jordan, M. A.; Wilson, L. *Nat. Rev. Cancer* **2004**, *4*, 253–265.
- (3) Beckers, T.; Mahboobi, S. *Drugs Future* **2003**, *28*, 767–785.
- (4) Gottesman, M. M. *Annu. Rev. Med.* **2002**, *53*, 615–627.
- (5) Bai, R.; Pettit, G. R.; Hamel, E. *J. Biol. Chem.* **1990**, *265*, 17141–17149.
- (6) Bai, R.; Durso, N. A.; Sackett, D. L.; Hamel, E. *Biochemistry* **1999**, *38*, 14302–14310.

- (7) Ayril-Kaloustian, S.; Zask, A. *Drugs Future* **2005**, *30*, 254–260.
- (8) Loganzo, F.; et al. *Cancer Res.* **2003**, *63*, 1838–1845.
- (9) Zask, A.; et al. *J. Med. Chem.* **2004**, *47*, 4774–4786.
- (10) Hamel, E.; Covell, D. G. *Curr. Med. Chem.: Anti-Cancer Agents* **2002**, *2*, 19–53.
- (11) Mitra, A.; Sept, D. *Biochemistry* **2004**, *43*, 13955–13962.
- (12) Schmitt, J.; Bernd, M.; Kutscher, B.; Kessler, H. *Bioorg. Med. Chem. Lett.* **1998**, *8*, 385–388.
- (13) Poncet, J.; Busquet, M.; Roux, F.; Pierre, A.; Atassi, G.; Jouin, P. *J. Med. Chem.* **1998**, *41*, 1524–1530.

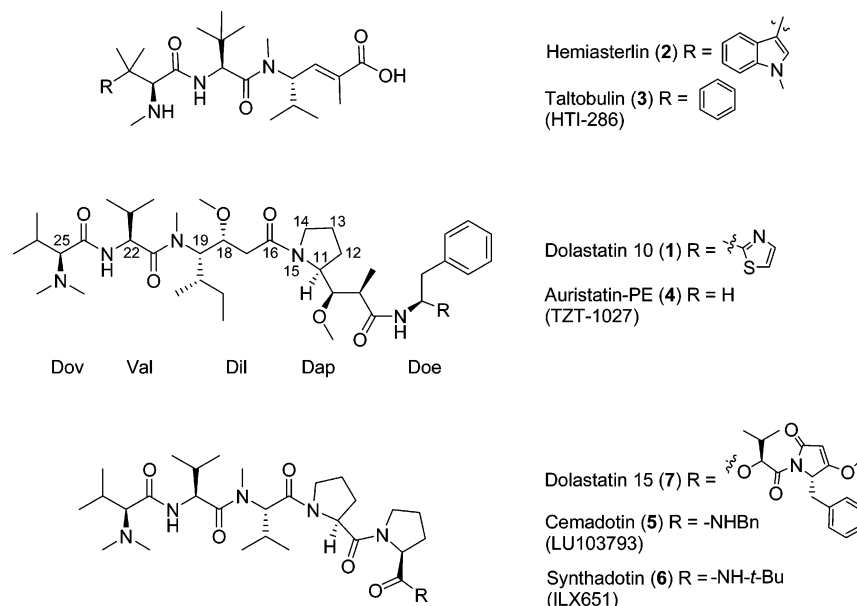


**Figure 1.** Peptidic antimicrotubule agents.

modeling study seeking to identify the tubulin binding site of these peptides, using molecular dynamics simulations and molecular docking studies, proposed overlapping structural regions, but could not provide a definitive binding pharmacophore among the peptides.<sup>11</sup> In another approach to identify functionality necessary for activity, preparation of simplified versions of dolastatin 15, by converting several of its amino acids into N-substituted glycines, failed to give active compounds.<sup>12</sup> A study, using similarities in the structures of dolastatin 10 and dolastatin 15 as a basis to design analogues in which their central amino acids (dolaisoleuine (Dil) and Me-Val-Pro, respectively) were interchanged, failed to show an equivalence of these units.<sup>13</sup> Our extensive SAR studies on **3** revealed critical elements necessary for potent cytotoxicity,<sup>9</sup> several of which translate to comparable moieties in the amino terminus tripeptide of the dolastatins, and thereby allowed us to overlay these seemingly disparate peptidic natural products. To experimentally establish a connection between the hemiasterlin tripeptides and the more complex dolastatins, we synthesized hybrids composed of hemiasterlin analogues coupled to the carboxy terminus dipeptides of the dolastatins. Herein we report our findings that these hybrids are potent antimicrotubule agents that overcome resistance associated with the P-glycoprotein transporter.

## Synthesis

Coupling of **3** to dolaproine-dolaphenine (Dap-Doe, **8**) using diethyl cyanophosphonate and triethylamine in dimethylformamide (DMF) gave the hybrid **9** (Scheme 1). Similarly, **3** was coupled to Dap-NHCH<sub>2</sub>CH<sub>2</sub>Ph (**10**) using 1-hydroxybenzotriazole hydrate (HOBT), 1-(3-dimethylaminopropyl)-3-ethylcarbodiimide (EDC), and 4-methylmorpholine in DMF to give the hybrid **11**. Coupling of **3** to Pro-Pro-NHBn (**12**) using HOBT, EDC, and Hunig's base in acetonitrile gave hybrid **13**. Tripeptide **14**<sup>14</sup> was coupled to L-proline benzylamide using HOBT, EDC, and 4-methylmorpholine in DMF to give the hybrid **15**.

## Results and Discussion

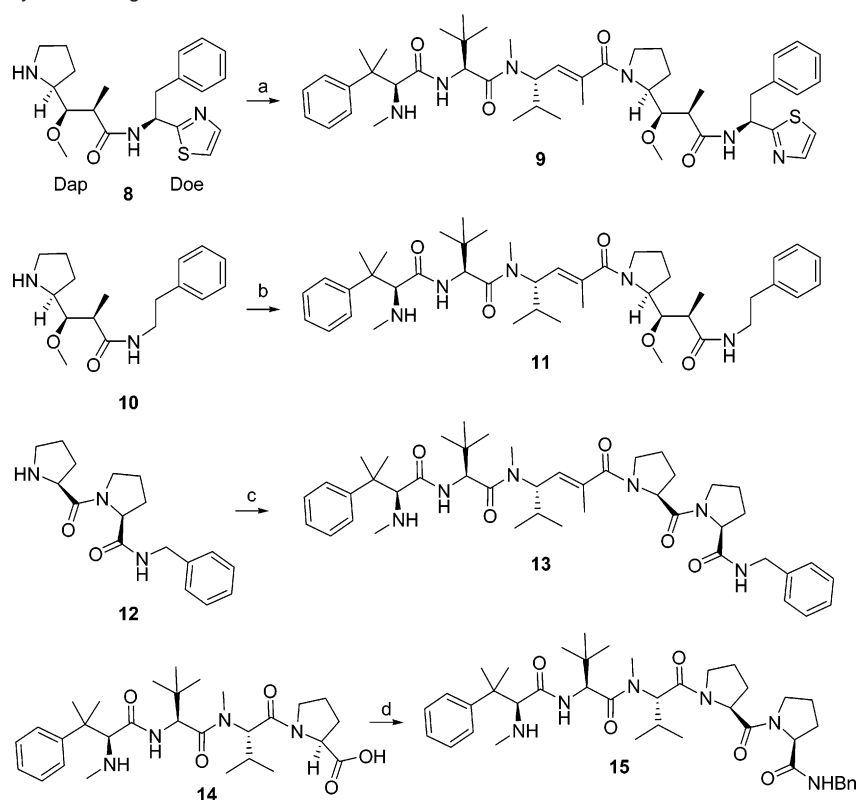
SAR studies<sup>9</sup> on **3** revealed several groups that were critical for activity and that correlated with moieties on the dolastatin 10 amino terminus tripeptide, dolavalline-valine-dolaisoleuine (Dov-Val-Dil) (Figure 1). The basic NHMe moiety of **3** was required as its replacement by methyl, ethyl, OMe, SMe, and SO<sub>2</sub>Me groups (**16a**, **16b**, **16c**, **16d**, and **16e**, respectively) led to a decrease in potency of 2–3 orders of magnitude relative to that of **3** (Figure 2, Table 1).<sup>9</sup> Removal of the NHMe group in **3** gave an analogue (**16f**) with an IC<sub>50</sub> of >3000 nM in the KB cells.<sup>9</sup> Similarly, neutralization of the NHMe group's basicity in **2** by acylation or quaternization led to an analogue 3–4 orders of magnitude less potent than **2** in human mammary carcinoma MCF-7 cells.<sup>15</sup> However, methylation to give analogue **17** with an NMe<sub>2</sub> group, as present in the dolastatins (position 25 of dolastatin 10), led to no significant loss of potency.<sup>9</sup> Similarly, replacement of the NMe<sub>2</sub> group with NHMe was tolerated in the corresponding amino acid (Dov) of dolastatin 10 (position 25).<sup>16</sup> With the importance of a basic nitrogen in **3** established and the presence of the same group in dolastatin 10, the backbones of the peptides could be aligned (Figure 3). A correspondence between the *tert*-butyl group of **3** and the Val isopropyl group at position 22 of dolastatin 10 is revealed through this overlay. Furthermore, in both **3** and dolastatin 10 good activities are achieved only if there is a high degree of branching at the  $\beta$ -carbon of the amino acid at this position. Thus, the potency of analogues of **3** (**18a–c**) decreased progressively from 5.2 to 48 to 381 nM in the KB-3-1 cells as the *tert*-butyl group was sequentially changed to less branched groups (isopropyl, ethyl, and methyl, respectively). Similarly, in dolastatin 10 a *sec*-butyl substituent at the corresponding position 22 led to an analogue that was more cytotoxic across a variety of cell lines than the analogue with a less branched isobutyl substituent.<sup>17</sup>

(14) Zask, A.; et al. *Bioorg. Med. Chem. Lett.* **2004**, *14*, 4353–4358.

(15) Nieman, J. A.; Coleman, J. E.; Wallace, D. J.; Piers, E.; Lim, L. Y.; Roberge, M.; Andersen, R. J. *J. Nat. Prod.* **2003**, *66*, 183–199.

(16) Poncet, J. *Curr. Pharm. Des.* **1999**, *5*, 139–162.

(17) Pettit, G. R. *Prog. Chem. Org. Nat. Prod.* **1997**, *70*, 1–79.

Scheme 1. Synthesis of Hybrid Analogues<sup>a</sup>

<sup>a</sup> Conditions and reagents: (a) **3**, diethyl cyanophosphonate, Et<sub>3</sub>N, DMF; (b) **3**, EDC, HOBT, 4-methylmorpholine, DMF; (c) **3**, EDC, HOBT, Hunig's base, CH<sub>3</sub>CN; (d) L-proline benzylamide, EDC, HOBT, 4-methylmorpholine, DMF.

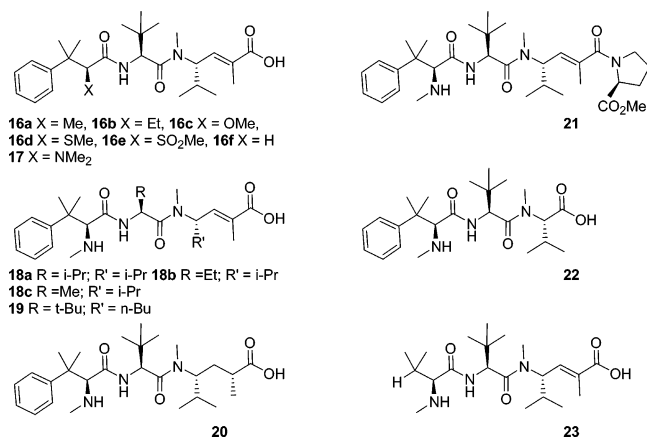


Figure 2. Taltobulin analogues. In **16b**, **16d**, and **16e** the chirality of the position bearing X is *R/S*.

Correspondence of the isopropyl group in **3** with the Dil isobutyl group at position 19 is substantiated by the SAR showing that longer substituents (e.g., *n*-butyl) are tolerated at this position in **3** (**19**) and that both peptides suffer a similar, approximately 2 orders of magnitude loss of cytotoxicity upon inversion of configuration (*S* to *R*) at this position.<sup>9,17</sup> The lack of an olefin in the Dap region of dolastatin 10 is consistent with retention of cytotoxicity upon saturation of the double bond in **3** (**20**),<sup>9</sup> provided that the configuration of the resulting aliphatic methyl group is *R*. The correct configuration (*R* and *S* at positions 18 and 19, respectively) is also important for activity in the saturated dolastatin 10 Dil unit.<sup>17</sup> Figure 3 shows a correspondence of the carboxylic acid in **3** with the amide group at positions 15 and 16 in dolastatin 10. This is substantiated by

Table 1. Taltobulin Analogues

compd	KB-3-1 <sup>a</sup>	KB-8-5 <sup>a</sup>	KB-V1 <sup>a</sup>	tubulin <sup>b</sup>
<b>3</b>	0.96	2.3	77	88
<b>16a</b>	561	639	>3000	94
<b>16b</b>	912	1202	5248	54
<b>16c</b>	1416	1229	>3000	54
<b>16d</b>	691	1148	>6000	79
<b>16e</b>	1750	2106	>3000	80
<b>16f</b>	>3000	>3000	>3000	21
<b>17</b>	1.6	3.7	116	93
<b>18a</b>	5.2	11	288	78
<b>18b</b>	48	70	1062	73
<b>18c</b>	381	902	>3000	8
<b>19</b>	36	78	>3000	52
<b>20</b>	8.5	19	1316	99
<b>21</b>	1.5	7.3	291	82

<sup>a</sup> IC<sub>50</sub> (nM) in cells. <sup>b</sup> Percent inhibition of tubulin polymerization at 0.3 μM.

the ability of the carboxylic acid of **3** to be converted to amides with retention of cytotoxicity.<sup>9</sup> Amide **21**, derived from coupling of **3** with proline methyl ester, is the most potent amide analogue found.<sup>14</sup> Significantly, the proline group in **21** correlates with the pyrrolidine ring of the Dap in dolastatin 10 at positions 11–15.

The above observations encouraged us to embark on a synthesis of hybrids of **3** and the dolastatins. We reasoned that the equivalence of the amino terminus tripeptide (e.g., Dov-Val-Dil) of the dolastatins with **3** would support a hybrid structure comprised of **3** and the carboxy terminus dipeptide (e.g., Dap-Doe) of the dolastatins. Biological activity of these hybrids would serve to establish the structural relationship between these two classes of natural products. Moreover, these

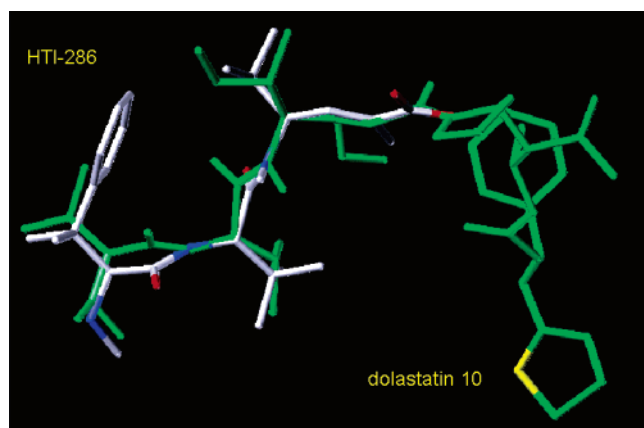


**Figure 3.** Superposition of minimum energy conformations of **1** and **3**. Minimum energy conformations were generated using the MMFF force field.

**Table 2.** Taltobulin/Dolastatin Hybrid Analogues

compd	KB-3-1 <sup>a</sup>	KB-8-5 <sup>a</sup>	KB-V1 <sup>a</sup>	KB-V1/KB-3-1 <sup>b</sup>	tubulin <sup>c</sup>
<b>13</b>	1.1	22	>3000	>2727	56
<b>15</b>	0.25	4.2	>3000	>12000	64
<b>7</b>	0.84	2.2	>3000	>3571	
<b>9</b>	0.75	4.1	180	240	62
<b>11</b>	0.90	5.1	191	212	69
<b>3</b>	0.96	2.3	77	80	88
<b>1</b>	0.073	0.34	43	589	78

<sup>a</sup> IC<sub>50</sub> (nM) in cells. <sup>b</sup> Ratio of IC<sub>50</sub> values. <sup>c</sup> Percent inhibition of tubulin polymerization at 0.3 μM.

hybrids have the potential to possess increased cytotoxic potency and reduced P-glycoprotein affinity relative to the parent compounds.

Synthesis of an initial hybrid analogue (**13**) combined **3** with the readily available **12**, which comprises the carboxy terminus dipeptide of the dolastatin 15 analogue cemadotin (**5**). Consistent with our hypothesis, the resulting hybrid **13** showed excellent activity in KB-3-1 cells (IC<sub>50</sub> = 1.1 nM), equipotent to taltobulin (**3**) and dolastatin 15 (**7**) (Table 2). However, susceptibility to the P-glycoprotein transporter increased dramatically relative to that of **3** as evidenced by the decreased potency of **13** versus the KB-8-5 and KB-V1 cells that express moderate and high levels of P-glycoprotein, respectively. The KB-V1/KB-3-1 ratio of >2727 for **13** is a relative measure of P-glycoprotein affinity, as the KB-3-1 cells do not express this transporter. Dolastatin 15 (**7**) is also a good ligand for P-glycoprotein as evidenced by its similarly high KB-V1/KB-3-1 ratio of >3571. With the proof of concept established, we next synthesized the dolastatin 10 and auristatin PE carboxy terminus dipeptides (**8** and **10**, respectively) according to the published routes<sup>18</sup> and coupled them with **3** to give the corresponding hybrids **9** and **11**, respectively (Table 2). These hybrid analogues were approximately as potent as **3** (IC<sub>50</sub> = 0.96 nM) in the KB-3-1 cells (**9**, IC<sub>50</sub> = 0.75 nM; **11**, IC<sub>50</sub> = 0.90 nM). Furthermore, they showed improved resistance to P-glycoprotein relative to dolastatin 10, as evidenced by a 2–3-fold lower KB-V1/KB-3-1 ratio. However, this ratio remained 2–3-fold higher than the ratio for **3**.

The amino terminus tripeptides of dolastatin 15 and its analogue cemadotin differ from that of dolastatin 10 in that the amino acid corresponding to Dil in dolastatin 10 is *N*-

methylvaline. To more fully explore the relationship between **3** and dolastatin 15, we used the truncated analogue of **3** in which the carboxy terminus was converted to *N*-methylvaline (**22**; KB-3-1, IC<sub>50</sub> > 3000 nM) (Figure 2).<sup>14</sup> Hybrid analogue **15**, composed of **22** and the carboxy terminus dipeptide (**12**) from cemadotin, had 3–4-fold higher potency in the KB-3-1 cells (IC<sub>50</sub> = 0.25 nM) than **3** or dolastatin 15 (**7**). Moreover, **15** had greater than 4-fold higher potency in the KB-3-1 cells than the analogous hybrid **13**, which combined **3** with **12**. However, in common with the other hybrids and the dolastatins, **15** was more susceptible to P-glycoprotein binding than **3** as evidenced by its dramatically reduced potency in the P-glycoprotein expressing KB-8-5 and KB-V1 cells (KB-V1/KB-3-1 > 12000).

In addition to their cytotoxic activity in the KB cell lines, the hybrid analogues inhibited cell-free tubulin polymerization with a potency comparable to that of taltobulin and dolastatin 10. Thus, analogues **9**, **11**, **13**, and **15** inhibited tubulin polymerization at a concentration of 0.3 μM by 56–69% (Table 2). In comparison, **3** and **1** inhibited tubulin polymerization at a concentration of 0.3 μM by 88% and 78%, respectively.

One key difference between the hemiasterlins and the dolastatins is the incorporation of an aromatic group in the amino terminus amino acid of the hemiasterlins. SAR studies of **3** showed that a group of sufficient lipophilicity at this position is a requirement for potent biological activity.<sup>9</sup> Indeed, the hemiasterlin analogue lacking a group at this position (**23**), as in the dolastatins, is greater than 3 orders of magnitude less cytotoxic than **3** in human mammary carcinoma MCF-7 cells.<sup>15</sup> Similarly, the *tert*-butyl ester of the amino terminus tripeptide of dolastatin 10 (Dov-Val-Dil) has been reported to lack potency (IC<sub>50</sub> > 1000 nM) in the inhibition of L1210 tumor cells.<sup>19</sup> The lipophilic aromatic groups in hemiasterlin and **3** obviate the need for the carboxy terminus dipeptide required for potency in the dolastatins, which lack an aromatic group. As a result, hemiasterlin and its analogues have decreased susceptibility to resistance mechanisms associated with P-glycoprotein expression as shown by their lower KB-V1/KB-3-1 ratios relative to the dolastatins.

In conclusion, we have established a structural relationship between the hemiasterlins and the dolastatins, two classes of naturally occurring peptidic antimicrotubule agents. Through the coupling of analogues of hemiasterlin (e.g., taltobulin) with the carboxy terminus dipeptide portions of the dolastatins, hybrid structures were successfully obtained which were potent anti-tumor agents, active in resistant cell lines. This information may be useful in the design of simpler analogues of the dolastatins with lower molecular weights and better activity in resistant cell lines expressing P-glycoprotein, or for establishing structural relationships with other naturally occurring peptidic antimicrotubule agents. The structural relationships among these peptidic natural products may also be useful in modeling studies seeking to establish a binding site in tubulin based on a common pharmacophore.

## Experimental Section

**Chemistry.** <sup>1</sup>H NMR spectra were determined with a Bruker DPX-300 spectrometer at 300 MHz. Chemical shifts (δ) are reported in parts per million relative to the peak for residual TMS (0 ppm) or dimethyl

(18) Shiori, T.; Hayashi, K.; Hamada, Y. *Tetrahedron* **1993**, *49*, 1913–1924.

(19) Bai, R.; Pettit, G. R.; Hamel, E. *Biochem. Pharm.* **1990**, *40*, 1859–1864.



sulfoxide (2.49 ppm) as an internal reference with coupling constants ( $J$ ) reported in hertz (Hz). The peak shapes are denoted as follows: s, singlet; d, doublet; t, triplet; q, quartet; m, multiplet; br, broad. Electrospray (ES) mass spectra were recorded in positive or negative mode on a Micromass Platform spectrometer. Electron impact and high-resolution mass spectra were obtained on a Finnigan MAT-90 spectrometer. Combustion analyses were obtained using a Perkin-Elmer Series II 2400 CHNS/O analyzer. Preparative reversed-phase HPLC was run on a Phenomenex Prodigy 5  $\mu$ M ODS column using a gradient solvent system. The term "concentrated" refers to removal of solvents using a rotary evaporator at water aspirator pressure with a bath temperature equal to or less than 60 °C. Reagents were obtained from commercial sources and were used without further purification.

**Biology.** The cellular cytotoxicity assays and cell-free tubulin polymerization assay were performed as described previously.<sup>8</sup>

***N*, $\beta$ , $\beta$ -Trimethyl-L-phenylalanyl-*N*<sup>1</sup>-[(1*S*,2*E*)-1-isopropyl-4-[(2*S*)-2-((1*R*,2*R*)-1-methoxy-2-methyl-3-oxo-3-[[1*S*]-2-phenyl-1-(1,3-thiazol-2-yl)ethylamino]propyl)pyrrolidin-1-yl]-3-methyl-4-oxobut-2-enyl]-*N*<sup>1</sup>,3-dimethyl-L-valinamide (9).** To a solution of **3** (0.094 g, 0.20 mmol) and (2*R*,3*R*,4*S*)-dolaproine-(*S*)-dolaphenine<sup>18</sup> (**8**; 0.066 g, 0.18 mmol) in dimethylformamide (1 mL) at 0 °C were added diethyl cyanophosphonate (33  $\mu$ L, 0.22 mmol) and triethylamine (31  $\mu$ L, 0.22 mmol). The reaction mixture was allowed to gradually warm to room temperature and then stirred for 60 h, and subsequently a few drops of water were added. The mixture was purified by reversed-phase HPLC, employing a gradient elution of 5% acetonitrile/95% water/0.1% trifluoroacetic acid to 100% acetonitrile over 1 h to give **9** as a white solid (0.084 g, 49%). HRMS (ESI):  $m/z$  calcd for C<sub>47</sub>H<sub>68</sub>N<sub>6</sub>O<sub>5</sub>S, 829.50447 (M + H)<sup>+</sup>; found, 829.5047. Anal. Calcd for C<sub>47</sub>H<sub>68</sub>N<sub>6</sub>O<sub>5</sub>S·2.00C<sub>2</sub>H<sub>2</sub>F<sub>3</sub>O<sub>2</sub>·H<sub>2</sub>O: C, 56.97; H, 6.75; N, 7.82. Found: C, 56.73; H, 6.64; N, 7.66. <sup>1</sup>H NMR (DMSO-*d*<sub>6</sub>):  $\delta$  (ppm) 0.77 (d, 6.40 Hz, 3 H), 0.86 (d, 6.40 Hz, 3 H), 0.99 (s, 9 H), 1.07 (d, 6.40 Hz, 3 H), 1.25 (s, 3 H), 1.39 (s, 3 H), 1.51–1.64 (m, 2 H), 1.65–1.74 (m, 2 H), 1.79 (s, 3 H), 1.88–2.02 (m, 1 H), 2.17–2.25 (m, 1 H), 2.29 (s, 3 H), 2.95 (s, 3 H), 2.98–3.22 (m, 3 H), 3.27 (s, 3 H), 3.38–3.46 (m, 2 H), 3.73 (dd, 9.57, 1.76 Hz, 1 H), 4.41 (d, 10.07 Hz, 1 H), 4.76 (d, 8.06 Hz, 1 H), 4.96 (t, 9.95 Hz, 1 H), 5.43 (m, 1 H), 5.53 (d, 8.56 Hz, 1 H), 7.12–7.54 (m, 11 H), 7.64 (d, 3.27 Hz, 1 H), 7.78 (d, 3.27 Hz, 1 H), 7.89 (br s, 1 H), 8.68 (t, 8.69 Hz, 2 H), 8.72–8.83 (br s, 1 H).

***N*-Methyl-3-phenyl-L-valyl-*N*<sup>1</sup>-[(1*S*,2*E*)-1-isopropyl-4-((2*S*)-2-((1*R*,2*R*)-1-methoxy-2-methyl-3-oxo-3-[[2-phenylethylamino]propyl)pyrrolidin-1-yl]-3-methyl-4-oxobut-2-enyl]-*N*<sup>1</sup>,3-dimethyl-L-valinamide (11).** To a solution of **3** (0.36 g, 0.77 mmol) and Dap-NHCH<sub>2</sub>-CH<sub>2</sub>Ph hydrochloride<sup>18</sup> (**10**; 0.31 g, 0.70 mmol) in DMF (5 mL) were added HOBT (0.19 g, 1.4 mmol), EDC (0.27 g, 1.4 mmol), and 4-methylmorpholine (0.15 mL, 1.4 mmol). The reaction mixture was stirred overnight at room temperature and then partitioned between diethyl ether and water. The aqueous phase was extracted three times with diethyl ether, and the combined extracts were washed once each with saturated aqueous sodium hydrogen carbonate and saturated aqueous sodium chloride. After being dried over anhydrous sodium sulfate, the organic phase was decanted and concentrated under reduced pressure to give a straw-colored foam (0.45 g), 150 mg of which was purified via reversed-phase HPLC, employing a gradient elution of 5% acetonitrile/95% water/0.1% trifluoroacetic acid to 100% acetonitrile over 1 h. A second HPLC purification was performed under the same conditions, but with 0.02% formic acid replacing 0.1% trifluoroacetic acid, to give **11** (0.16 g) as a white powder. MS:  $m/z$  746.4 (M + H)<sup>+</sup>. Anal. Calcd for C<sub>44</sub>H<sub>67</sub>N<sub>5</sub>O<sub>5</sub>·1.2CF<sub>3</sub>CO<sub>2</sub>H: C, 63.12; H, 7.79; N, 7.93. Found: C, 62.76; H, 7.88; N, 7.83. <sup>1</sup>H NMR (DMSO-*d*<sub>6</sub>):  $\delta$  (ppm) 0.75 (d, 6.8 Hz, 3 H), 0.86 (d, 6.4 Hz, 3 H), 0.98 (s, 9 H), 1.05 (d, 6.80

Hz, 3 H), 1.24 (s, 3 H), 1.37 (s, 3 H), 1.48–2.23 (m, 9 H), 1.80 (s, 3 H), 2.51 (s, 3 H), 2.72 (t, 7.2 Hz, 2 H), 2.94 (s, 3 H), 3.19–3.38 (m, 4 H), 3.32 (s, 3H), 3.77 (d, 9.2 Hz, 1 H), 3.80–3.88 (m, 1 H), 4.76 (d, 8.4 Hz, 1 H), 4.96 (t, 10.0 Hz, 1 H), 5.57 (d, 9.2 Hz, 1 H), 7.12–7.54 (m, 11 H), 7.88 (t, 5.54 Hz, 1 H), 8.51–8.95 (br s, 1 H).

**1-[(2*E*,4*S*)-2,5-Dimethyl-4-[methyl(*N*-methyl-3-phenyl-L-valyl-3-methyl-L-valyl)amino]hex-2-enoyl]-*D*-prolyl-*N*-benzyl-*D*-prolinamide (13).** To a solution of **3** (0.53 mmol, 250 mg) in acetonitrile (25 mL) was added HOBT (85 mg) followed by EDC (135 mg). After 21 h Hunig's base (0.37 mL) and 1-(pyrrolidine-2-carbonyl)pyrrolidine-2-carboxylic acid benzylamide (**12**; 1.59 mmol, 0.66 g) in acetonitrile (~3 mL) was added. After 2 h the reaction mixture was concentrated in vacuo and a portion purified by HPLC (20% H<sub>2</sub>O/20% CH<sub>3</sub>CN/0.1% trifluoroacetic acid to 100% CH<sub>3</sub>CN over 50 min) to give **13** as a white powder (60 mg). HRMS (ESI):  $m/z$  calcd for C<sub>44</sub>H<sub>64</sub>N<sub>6</sub>O<sub>5</sub>, 757.50203 (M + H)<sup>+</sup>; found, 757.50073. Anal. Calcd for C<sub>44</sub>H<sub>64</sub>N<sub>6</sub>O<sub>5</sub>·0.8CF<sub>3</sub>CO<sub>2</sub>H: C, 64.57; H, 7.70; N, 9.91. Found: C, 64.65; H, 7.48; N, 10.01. Analytical HPLC (YMC Pack Pro C18, 4.6 × 150 mm, gradient 0.02% formic acid/water to 0.02% formic acid/acetonitrile over 35 min, 1 mL/min, UV 215 nM, RT = 14.0 min, 98.0%). <sup>1</sup>H NMR (DMSO-*d*<sub>6</sub>):  $\delta$  (ppm) 0.735 (d, 3H, 6.3 Hz), 0.837 (d, 3H, 6.4 Hz), 0.975 (s, 9H), 1.228 (s, 3H), 1.335 (s, 3H), 1.770 (2, 3H), 1.64–2.23 (m, 14H), 2.971 (s, 3H), 3.36–3.73 (m, 4H), 4.191 (dd, 1H, 5.5 Hz, 15.5 Hz), 4.30–4.38 (m, 2H), 4.53–4.60 (m, 1H), 4.725 (d, 1H, 8.2 Hz), 4.937 (t, 1H, 10 Hz), 5.670 (d, 1H, 9.1 Hz), 7.18–7.40 (m, 8H), 7.41–7.49 (m, 2H), 8.277 (t, 1H, 6.4 Hz).

***N*, $\beta$ , $\beta$ -Trimethyl-L-phenylalanyl-3-methyl-L-valyl-*N*-methyl-L-valyl-L-prolyl-*N*-benzyl-L-prolinamide (15).** To a mixture of **14**<sup>14</sup> (0.11 g, 0.15 mmol) and L-proline benzylamide hydrochloride (0.18 g, 0.76 mmol) in DMF (2.5 mL) were added HOBT (0.11 g, 0.80 mmol), EDC (0.15 g, 0.80 mmol), and 4-methylmorpholine (0.13 mL, 1.2 mmol). The reaction mixture was stirred overnight at room temperature and then purified via reversed-phase HPLC, employing a gradient elution of 5% acetonitrile/95% water/0.1% trifluoroacetic acid to 100% acetonitrile over 1 h to give **15** as a pale yellow foam (0.12 g, 86%). HRMS (ESI):  $m/z$  calcd for C<sub>41</sub>H<sub>60</sub>N<sub>6</sub>O<sub>5</sub>, 717.46980 (M + H)<sup>+</sup>; found, 717.4697. Anal. Calcd for C<sub>41</sub>H<sub>60</sub>N<sub>6</sub>O<sub>5</sub>·2.00C<sub>2</sub>H<sub>2</sub>F<sub>3</sub>O<sub>2</sub>: C, 57.19; H, 6.61; N, 8.89. Found: C, 56.75; H, 6.76; N, 8.89. <sup>1</sup>H NMR (DMSO-*d*<sub>6</sub>):  $\delta$  (ppm) 0.74 (d, 6.8 Hz, 3 H), 0.88 (d, 6.4 Hz, 3 H), 1.01 (s, 9 H), 1.25 (s, 3 H), 1.38 (s, 3 H), 1.79–2.17 (m, 8H), 2.29 (s, 3 H), 3.10 (s, 2 H), 3.54–3.64 (m, 5 H), 4.05 (br s, 2 H), 4.16 (d, 5.6 Hz, 1 H), 4.20 (d, 5.2 Hz, 1 H), 4.32–4.36 (m, 1 H), 4.40 (d, 9.6 Hz, 1 H), 4.51–4.53 (m, 1 H), 4.78 (d, 7.6 Hz, 1 H), 5.05 (d, 11 Hz, 1 H), 7.20–7.50 (m, 10 H), 7.88 (br s, 1H), 8.28 (dd, 5.6 Hz, 6.0 Hz, 1H), 8.69 (d, 7.6 Hz, 1H), 8.75 (br s, 1H).

**Acknowledgment.** We thank the Pearl River Discovery Analytical Chemistry HPLC group for developing preparative methods for the purification of these analogues and Dr. Semiramis Ayral-Kaloustian and Dr. Lee Greenberger for their helpful discussions concerning this work. We thank Dr. Malini Ravi for help with the molecular modeling of Figure 3 and Dr. Carl Beyer for testing these compounds in the cell-free tubulin polymerization assay.

**Supporting Information Available:** Complete citations for refs 8, 9, and 14. This material is available free of charge via the Internet at <http://pubs.acs.org>.

JA053663V